

1 Light absorption of brown carbon aerosol in the PRD region of 2 China

3
4 J.-F. Yuan, X.-F. Huang, L.-M. Cao, J. Cui, Q. Zhu, C.-N. Huang, Z.-J. Lan, and L.-Y.
5 He

6
7 *Key Laboratory for Urban Habitat Environmental Science and Technology, School of Environment and Energy,*
8 *Peking University Shenzhen Graduate School, Shenzhen 518055, China*

9 Corresponding author. Tel.: +86 755 26032532; Fax: +86 755 26035332.

10 E-mail address: huangxf@pku.edu.cn (X.-F. Huang).

11
12 **Abstract:** The strong spectral dependence of light absorption of brown carbon (BrC) aerosol is
13 regarded to influence aerosol's radiative forcing significantly. The Absorption Angstrom Exponent
14 (AAE) method has been widely used in previous studies to attribute light absorption of BrC at
15 shorter wavelengths for ambient aerosols, with a theoretical assumption that the AAE of “pure”
16 black carbon (BC) aerosol equals to 1.0. In this study, the previous AAE method was improved by
17 statistical analysis and applied to both urban and rural environments in the Pearl River Delta (PRD)
18 region of China. A three-wavelength photo-acoustic soot spectrometer (PASS-3) and aerosol mass
19 spectrometers (AMS) were used to explore the relationship between the measured AAE and the
20 relative abundance of organic aerosol to BC. The regression and extrapolation analysis revealed
21 that more realistic AAE values for “pure” BC aerosol (AAE_{BC}) were 0.86, 0.82, and 1.02 between
22 405 and 781 nm, and 0.70, 0.71, and 0.86 between 532 and 781 nm, in the campaigns of
23 urban_{winter}, urban_{fall}, and rural_{fall}, respectively. Roadway tunnel experiments were conducted and
24 the results further confirmed the representativeness of the obtained AAE_{BC} values for the urban
25 environment. Finally, the average light absorption contributions of BrC (\pm relative uncertainties)
26 at 405 nm were quantified to be 11.7% ($\pm 5\%$), 6.3% ($\pm 4\%$), and 12.1% ($\pm 7\%$) in the campaigns of
27 urban_{winter}, urban_{fall}, and rural_{fall}, respectively, and those at 532 nm were 10.0% ($\pm 2\%$),
28 4.1% ($\pm 3\%$), and 5.5% ($\pm 5\%$), respectively. The relatively higher BrC absorption contribution at
29 405 nm in the rural_{fall} campaign could be reasonably attributed to the biomass burning events
30 nearby, which was then directly supported by the biomass burning simulation experiments
31 performed in this study. This paper indicates that the BrC contribution to total aerosol light
32 absorption at shorter wavelengths is not negligible in the highly urbanized and industrialized PRD
33 region.

34
35 **Key words:** Brown carbon (BrC), Black carbon (BC), Light absorption, Absorption Angstrom
36 Exponent (AAE)

37 38 1. Introduction

39
40 Light absorbing carbonaceous aerosols including black carbon (BC) and brown

41 carbon (BrC) are the primary matters absorbing light in the atmosphere. The
42 importance of BC has been widely recognized in recent decades due to its effects of
43 radiative forcing on climate change, while the role of BrC is far from being well
44 known (Jacobson, 2001; Hansen et al., 1997; Haywood et al., 1997; Ramanathan and
45 Carmichael, 2008; Gadhavi and Jayaraman, 2010; Wang et al., 2014). BrC is organic
46 carbon which can absorb light based on a variety of chemical structures like
47 nitrated/polycyclic aromatics, phenols, humic-like substances and biopolymers, etc.
48 (Jacobson MZ, 1999; Sun et al., 2011; Poschl, 2005). Main sources of BrC include
49 biomass and biofuel burning, atmospheric humic-like substances (HULIS) from
50 multiple phase actions, and photochemical oxidation of volatile organic compounds
51 (VOCs) (Bond, 2001; Bergstrom et al., 2007; Alexander et al., 2015). South and East
52 Asia are typical regions of atmospheric brown clouds (ABC) (Alexander et al., 2015).
53 Biomass burning has been recognized as a significant contributor to ABC, including
54 forest burning, crop waste burning, traditional religious activities and residential
55 burning in those countries like India, China, Thailand, etc. (Venkataraman et al., 2006;
56 Yan et al., 2006; Chakrabarty et al., 2013; Chakrabarty et al., 2014; Huang et al.,
57 2012). BrC mainly absorbs light at UV and short-visible wavelengths (Chen and Bond,
58 2010; Kirchstetter et al., 2004; Lewis et al., 2008; Sandradewi et al., 2008; Schmid et
59 al., 2006) and this strong spectral dependence has aroused more and more interest
60 recently (Feng et al., 2013; Bahaduret al., 2012; Chung et al., 2012b; Wang et al.,
61 2014; Jethva et al., 2011). BrC was ever estimated to contribute about 10–30% of
62 total absorption of fine particles at shorter wavelengths, e.g., at 365 and 405 nm, and
63 contribute approximately 10% at mid-visible wavelengths, e.g., at 532 nm (Bahadur et
64 al., 2012; Lack et al., 2012b; Washenfelder et al., 2015; Nakayama et al., 2014).
65 During an agricultural waste burning event, BrC aerosol could contribute more than
66 65% of light absorption at 370 nm and 15% at a mid-wavelength (Favez et al., 2009).
67 However, the complexity and variety of molecular composition of BrC and the
68 mixing state with other substances make it very challenging to study BrC optical
69 properties (Alexander et al., 2015). Extensive experimental data from field studies are
70 essential to evaluate light absorption by BrC as well as constraining and validating
71 atmospheric and climate models.

72

73 There were two main methods to identify the absorption of BrC in total aerosol
74 absorption at shorter wavelengths in previous studies: one was to use theoretical Mie
75 models to calculate the light absorption of BrC with input of ambient chemical,
76 physical, and optical measurements of bulk aerosol (Lack et al., 2012b); the other was
77 based on optical measurement followed by absorption angstrom exponent (AAE)
78 calculation, which was actually simpler and widely used with a criterion of AAE for
79 “pure” BC aerosol (AAE_{BC}) (Clarke et al., 2007; Favez et al., 2009; Yang et al., 2009;
80 Bahadur et al., 2012; Chung et al., 2012a). The AAE_{BC} has been commonly assumed
81 to be 1.0 theoretically in many studies, but this simple assumption may not be reliable,
82 and could cause a possible bias of the attributed absorption of BC from -22% to +7%
83 and then cause significant uncertainty of attributed BrC absorption (Lack and
84 Langridge, 2013).

85

86 Some previous studies showed that ambient AAE was significantly affected by
87 aerosol OC/EC (organic carbon/elemental carbon) ratio, suggesting a potentially
88 important role of organic matter in aerosol light absorption (Utry et al., 2014). In this
89 study, we tried to improve the AAE method through statistical analysis based on
90 on-line measurements in field campaigns. The improved AAE method was applied to
91 both urban and rural areas in the Pearl River Delta (PRD) region of China, in order to
92 attribute the light absorption of BrC there. The PRD region is one of the three
93 economically-developed regions of China and has been considered as one of the
94 world’s largest sources of anthropogenic soot emissions (Streets et al., 2001; Bond et
95 al., 2004; Koch and Hasen, 2005). Despite of strong emissions of BC aerosol in the
96 highly urbanized and industrialized PRD region, the light absorption contribution of
97 BrC aerosol should not be neglected without effective evaluation. Therefore, the focus
98 of this paper is to reasonably quantify the light absorption of BrC aerosol in PRD with
99 effective uncertainty evaluation using an improved AAE method.

100

101 2. Experimental and data analysis methods

102 2.1 Sampling sites and periods

103

104 Our measurements contained three field campaigns conducted in Shenzhen and
105 Heshan in PRD during fall and winter, which are usually the polluted dry seasons of
106 PRD with high frequency of haze episodes. The Shenzhen site (SZ) was an urban site
107 in the southeast of the PRD region. It was on the campus of Peking University
108 Shenzhen Graduate School (22.60°N, 113.97°E), located in the west of Shenzhen, and
109 the sampling periods were from 15th January to 19th February in the winter
110 (urban_winter) and from 12th September to 9th October in the fall (urban_fall) in 2014.
111 The Heshan site (HS) was a rural site (22.71°N, 112.93°E), 40–50 km southwest to
112 the megacity of Guangzhou in the central PRD. It was located on the top of a small
113 hill with little local fossil fuel combustion emission nearby except biomass burning.
114 The HS sampling period was from 1st to 22th November in the fall (rural_fall) in 2014
115 and biomass burning events were observed occasionally as an obvious anthropogenic
116 source in the nearby farmland.

117

118 In addition, tunnel experiments were also performed in Shenzhen in 2014 to explore
119 the AAE values in a highly BC-polluted environment. We performed tunnel
120 experiments three times in Shenzhen urban areas: twice in the Tanglangshan tunnel
121 (TL) and once in the Jiuweiling (JW) tunnel. The sampling periods of the
122 Tanglangshan tunnel were from 0:00 am to 5:30 am on both 16th and 18th October (as
123 the TL-1 and TL-2 experiments, respectively). The TL tunnel was 1.71 km in length
124 with two channels that has three lanes in one direction for traffic, and the driving
125 speeds in the tunnel were usually between 50–60 km/h. The monitoring car was
126 located 400 m in depth from the entrance. The sampling period of the JW tunnel was
127 from 3:30 pm to 24:00 pm on 10th December (as the JW experiment). The JW tunnel
128 was 1.45 km in length with two channels that has two lanes in one direction for traffic,
129 and the driving speeds in the tunnel were usually about 60 km/h. The monitoring car
130 was located 800 m in depth from the entrance.

131

132 Moreover, since biomass burning is recognized as an important source of BrC
133 (Ramanathan, et al., 2007) and is a popular source in rural areas in PRD, especially
134 during the harvest season (He et al., 2011; Zhang et al., 2013), we performed biomass
135 burning simulation experiments in a combustion laboratory to study the spectral
136 dependence of aerosol light absorption in biomass burning smoke. Different types of
137 biomass materials, including straw, deciduous leaf, and firewood, were burned in two
138 different combustion modes, i.e., stove burning and open burning, to simulate the
139 traditional residential and field biomass burning. The combustion system in the
140 laboratory included four parts: combustion simulation, dilution, tube sampling, and
141 instrumental analyzing. The stove was built with bricks and mortar according to the
142 local traditional structure. More detailed information of the combustion system was
143 described in our previous paper (He et al., 2010). Different biomass materials were
144 burned inside the stove to simulate a complete water heating process referring to a
145 standard protocol of water boiling test provided by the University of California
146 (<http://www.aprovecho.org/lab/pubs/testing>). In addition, a certain amount of straw
147 was piled up and burned on a pallet made of iron wire to simulate open burning of
148 crop residues in the field.

149

150 2.2 Instrumentation

151

152 For the ambient sampling in this study, the instruments were placed in a temperature
153 controlled room (or a monitoring car for the tunnel experiments), and the outdoor air
154 was induced through a PM_{2.5} cyclone inlet placed on the rooftop and then dried before
155 it entered the inlets of the instruments. A three-wavelength Photo-acoustic Soot
156 Spectrometer (PASS-3) (Droplet Measurement Technologies, CO, USA) was used to
157 measure light absorption at 405, 532, and 781 nm with a data output time resolution
158 of 2 min. The principles and technical details of PASS-3 were described previously by
159 Arnott et al. (1999). Then, we processed the 2 min time resolution data of absorption
160 at three wavelengths for half hour averages and made further data analysis based on
161 the half hour time resolution datasets. On the other hand, we also processed the 10
162 min time resolution data of organic aerosol derived from AMS or ACSM for half hour

163 averages to explore the relationship with the absorption datasets.

164

165 A high-resolution time-of-flight aerosol mass spectrometer (HR-ToF-AMS)
166 (Aerodyne Research, MA, US) was used to measure non-refractory species of PM₁
167 including organic aerosol with a time resolution of 10 min at the SZ site. The detailed
168 description of the instrument was given by DeCarlo et al. (2006), and the calibration
169 followed the standard protocols (Jayne et al., 2000; Jimenez et al., 2003; Drewnick et
170 al., 2005). More details about the HR-ToF-AMS operation were described in our
171 previous publications (He et al., 2011; Huang et al., 2011). An aerosol chemical
172 speciation monitor (ACSM) (Aerodyne Research, MA, US) was used at the HS site
173 and in the tunnel experiments with a time resolution of 10 min. In comparison with
174 HR-ToF-AMS, ACSM was smaller and more convenient to be transported to field
175 sampling sites and setup in a monitoring car with limited space. The detailed
176 description of ACSM was given by Ng et al. (2011).

177

178 2.3 Calibration of PASS-3

179

180 The calibrations of PASS-3 for flow rate, laser power, and absorption were conducted
181 following the standard procedures provided by the operational manual, which were
182 also applied in relevant previous studies (Arnott et al., 2000; Lan et al., 2013;
183 Nakayama et al., 2015). Firstly, the flow rate of sample air was calibrated by a soap
184 film flow meter, with the results shown in Table 1; secondly, the laser power for each
185 wavelength was calibrated by a laser power meter and the error in Table 1 indicated
186 the reading difference between the laser power meter and the laser detector inside the
187 instrument; thirdly, the light absorption calibration was performed by measuring
188 highly absorbing NO₂ (200 ppm) at 532 nm. Then a good linear regression (with
189 $R^2 > 0.99$) of the calculated extinction coefficient of NO₂ and the measured light
190 absorption was established. Since the scattering of gas is negligible, the extinction of
191 NO₂ should be very close to the absorption of NO₂, and thus the slope of the fitting
192 curve should be very close to 1, as shown in Table 1. The detection limit of aerosol

193 light absorption with 2 s time resolution was 10, 10, and 3 Mm⁻¹ at 405, 532, and 781
 194 nm, respectively.

195 **Table 1.** The calibration results of PASS-3 in the campaigns.

Campaign	Flow rate (lpm)	Error of laser power_405 nm	Error of laser power_532 nm	Error of laser power_781 nm	Slope (R^2)
Urban _{winter}	0.97	0.6 (%)	2.3 (%)	2.5 (%)	1.02 (0.995)
Urban _{fall}	0.98	4.0 (%)	1.1 (%)	0.9 (%)	1.03 (0.996)
Rural _{fall}	0.98	2.5 (%)	5.0 (%)	3.6 (%)	1.04 (0.993)
Tunnel	0.98	2.8 (%)	4.3 (%)	3.7 (%)	1.07 (0.993)

196

197 2.4 Calculation of AAE and light absorption of BrC

198

199 The AAE is an application of Angstrom exponent (Angstrom, 1929) to describe the
 200 wavelength dependence of visible light absorption by aerosol, as expressed in
 201 Equation 1:

$$202 \text{ AAE} = -\ln(\text{Abs}_{\lambda_1}/\text{Abs}_{\lambda_2})/\ln(\lambda_1/\lambda_2) \quad (1)$$

203 Where Abs can be obtained by the absorption measurement and λ represents a
 204 wavelength. The traditional AAE method for estimating BrC light absorption was
 205 described previously by Lack and Langridge (2013), and it can be expressed in
 206 Equations 2 and 3:

$$207 \text{ BC_Abs}_{\lambda_1} = \text{Abs}_{\lambda_2} \times (\lambda_2/\lambda_1)^{\text{AAE}_{\text{BC}}} \quad (2)$$

$$208 \text{ BrC_Abs}_{\lambda_1} = \text{Abs}_{\lambda_1} - \text{BC_Abs}_{\lambda_1} \quad (3)$$

209 Where Abs_{λ_2} is the measured absorption at a longer wavelength, at which BrC has
 210 negligible or no absorption. $\text{BC_Abs}_{\lambda_1}$ is the attributed absorption of BC at a shorter
 211 wavelength. $\text{BrC_Abs}_{\lambda_1}$ is thus the attributed absorption of BrC at the shorter
 212 wavelength. AAE_{BC} is referred to as the AAE caused solely by “pure” BC aerosol,
 213 and is usually assumed to be 1.0 theoretically. The total uncertainty of $\text{BrC_Abs}_{\lambda_1}$
 214 calculated (U_t) thus arises from both the absorption measurements and the AAE
 215 attribution method, and can be estimated by Equation 4:

$$U_t = \sqrt{(U_{Abs_{\lambda 1}})^2 + (U_{Abs_{\lambda 2}})^2 + (U_{AAE_BC} \times \ln(\lambda_2/\lambda_1))^2} \quad (4)$$

Where $U_{Abs_{\lambda 1}}$ and $U_{Abs_{\lambda 2}}$ are the relative uncertainties of the absorption measured at λ_1 and λ_2 , respectively; U_{AAE_BC} is the absolute uncertainty of the AAE_{BC} used, and needs to be multiplied by $\ln(\lambda_2/\lambda_1)$ to obtain the relative uncertainty of the AAE method. The uncertainty of the absorption measurement at a wavelength ($U_{Abs_{\lambda}}$) includes the fit to the absorption calibration slope, the electronic noise within the instrument (Lack et al., 2012a), as well as the drift correction of signals, and can be expressed as below:

$$\Delta X = \sqrt{(\Delta X_{calibration})^2 + (\Delta X_{noise})^2 + (\Delta X_{drift})^2} \quad (5)$$

$$U_{Abs_{\lambda}} = \Delta X / Abs_{\lambda} \quad (6)$$

Where $\Delta X_{calibration}$ is derived from the uncertainty of the regression slope under a 95% confidence level (p); ΔX_{noise} can be calculated through uncertainty propagation of noise equivalent absorption measured by PASS-3 every 2 minutes; ΔX_{drift} is the standard deviation of the averaged baseline absorption of filtered air. Finally, ΔX is divided by Abs_{λ} to get the corresponding relative uncertainty ($U_{Abs_{\lambda}}$). In result, the relative uncertainties of the absorption measurements at the three wavelengths were ~1.2% for the campaign of urban_{winter}, 0.8–0.9% for the campaign of urban_{fall}, and 1.5–1.6% for the campaign of rural_{fall}.

234

235 3. Results and discussion

236

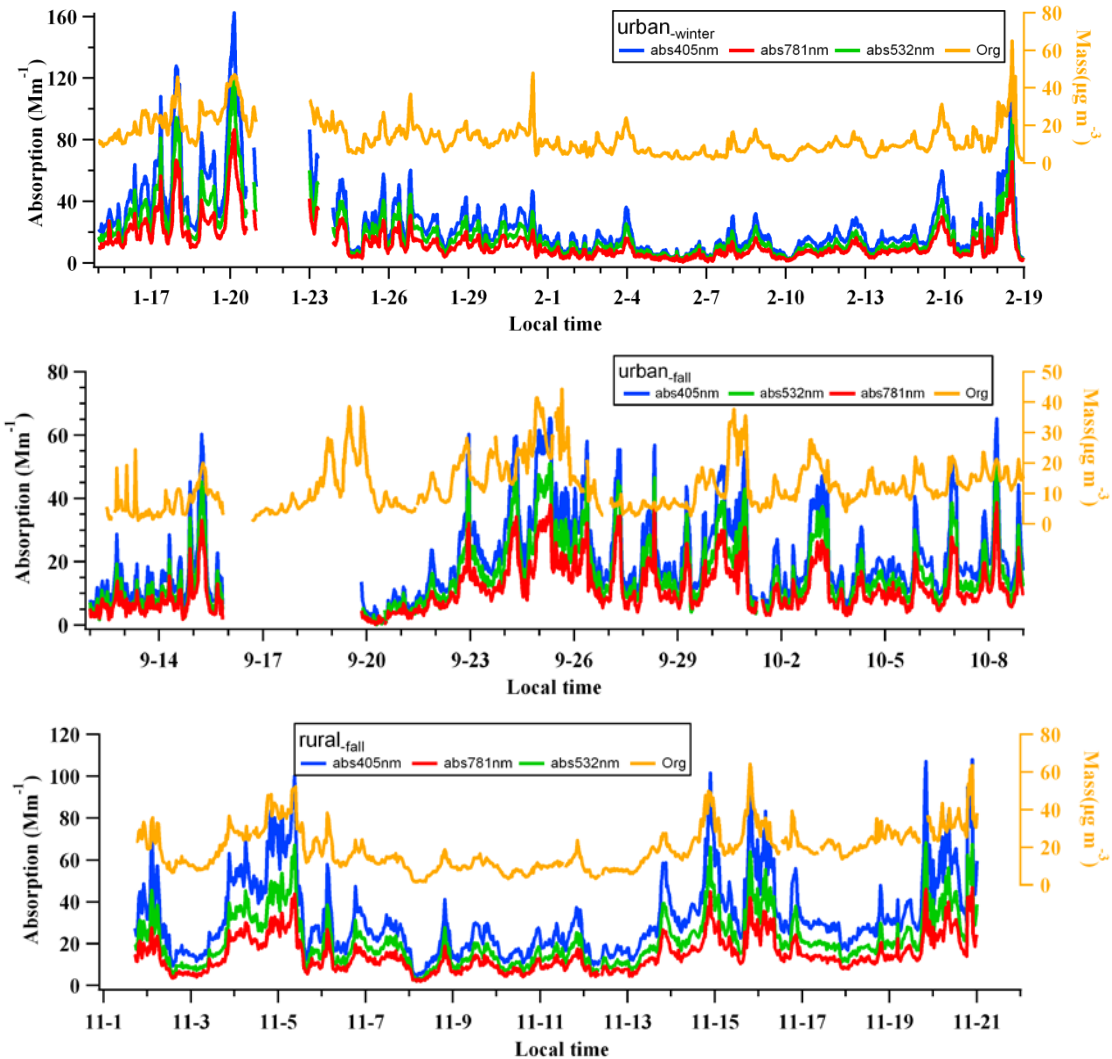
237 3.1 Aerosol light absorption

238

239 The time series of PM_{2.5} light absorption at three wavelengths in different campaigns
 240 were shown in Fig.1. In the urban_{winter} campaign, the average absorption was 25.6,
 241 18.7, and 12.9 Mm⁻¹ at 405, 532, and 781 nm, respectively. In the urban_{fall} campaign,
 242 the average absorption was 21.6, 16.2, and 11.8 Mm⁻¹ at 405, 532, and 781 nm,
 243 respectively. It was seen that the aerosol absorbed more light in the winter, and its

244 maximum absorptions were 162, 122, and 86.6 Mm^{-1} at 405, 532, and 781 nm,
245 respectively, more than two times of the maximum values in the fall. The higher
246 aerosol pollution observed in the winter could be attributed to the unfavorable
247 meteorological conditions in PRD in the winter, when the air mass came from the
248 polluted northern continent with a overwhelming frequency and the atmospheric
249 boundary layer became shallower due to lower ambient temperatures (Huang et al.,
250 2014). In the rural_{-fall} campaign, the average absorption was 32.5, 21.5, and 14.6 Mm^{-1}
251 at 405, 532, and 781 nm, respectively, which were even higher than those of the
252 urban_{-winter} and urban_{-fall} campaigns, but this was not strange since HS was a receptor
253 site, suffering from the polluted air outflow from the northeast, where the megacity of
254 Guangzhou was located, during the fall and winter seasons (Gong et al., 2012). The
255 campaign-average ambient AAE_{405_781} values (\pm relative uncertainties) were
256 calculated to be 1.05 ($\pm 0.01\%$), 0.92 ($\pm 0.10\%$), and 1.22 ($\pm 0.002\%$), respectively,
257 for the urban_{-winter}, urban_{-fall}, and rural_{-fall} campaigns, while those of AAE_{532_781} were
258 0.98 ($\pm 0.01\%$), 0.82 ($\pm 0.05\%$), and 1.00 ($\pm 0.001\%$), respectively. The
259 corresponding uncertainties in the brackets were calculated through the uncertainty
260 propagation of the absorption measurement uncertainties based on Equation 1. The
261 relatively higher values of AAE_{405_781} and AAE_{532_781} in the rural_{-fall} campaign might
262 be related to the biomass burning in the farmland surrounding the HS site.

263



264

265 **Fig.1.** The time series of aerosol light absorption and mass concentration of organic aerosol in the
 266 different campaigns.

267

268 It should be noted here that the contribution of dust particles to the aerosol light
 269 absorption was considered to be negligible in this study. Firstly, there was no dust
 270 event during the three campaigns; secondly, organic aerosol typically contributes >30%
 271 of PM_{2.5} mass in both urban and rural environments, far higher than that of the dust
 272 (<5%) (Huang et al., 2014). Considering that the mass absorption efficiency (MAE)
 273 values of dust at shorter and mid-visible wavelengths are lower than those of organic
 274 aerosol by a magnitude of one or two (Favez et al., 2009; Yang et al., 2009), the light
 275 absorption contribution of dust could be negligible in comparison with that of organic
 276 aerosol in PRD. Therefore, light absorption of dust was not taken into account in the

277 following discussion.

278

279 3.2 Determination of the AAE for “pure” BC aerosol

280

281 Theoretically, the AAE for “pure” BC aerosol (AAE_{BC}) is assumed to be 1.0 (Lack
282 and Langridge, 2013), and BrC absorption at shorter wavelengths can raise this value
283 in ambient atmosphere. In this study, we explored more realistic AAE_{BC} in PRD by
284 establishing a univariate regression relationship for each campaign, as shown in Fig. 2.
285 In each campaign, the organic aerosol mass concentration was measured by AMS or
286 ACSM, and the absorption at 781 nm (Abs_{781nm}) could be used to represent the BC
287 amount since BrC had negligible absorption at longer wavelengths (Kirchstetter et al.,
288 2004; Lack and Langridge, 2013; Lack et al., 2012b). Then, $r_{org/bc}$ (the ratio of
289 organic aerosol mass concentration to Abs_{781nm}) was used as an index of the relative
290 abundance of organic aerosol to BC. Finally, the AAE_{405_781} and AAE_{532_781} were
291 plotted versus the $r_{org/bc}$ averaged within equal intervals for each campaign in Fig. 2,
292 with the corresponding linear fitting curves.

293

294 For all the campaigns, the linear relationships between AAE_{405_781} (or AAE_{532_781}) and
295 $r_{org/bc}$ were significant enough with correlation coefficients (R^2) of 0.59–0.98,
296 indicating AAE was positively related with the relative amount of organic matter,
297 which certainly included BrC. Utry et al. (2014) also revealed a strong correlation
298 between AAE and aerosol OC/EC at an urban site in Hungary, where OC was mainly
299 emitted from wood burning and contained a large amount of BrC. The intercepts of
300 the fitting curves in Fig.2, where $r_{org/bc}=0$, can be regarded as the situation for “pure”
301 BC without any organic matter, and thus are suitable proxies of the AAE_{BC} values for
302 the different campaigns. The uncertainties of the regression intercepts represent the
303 absolute uncertainties of the AAE_{BC} ($U_{AAE_{BC}}$), and can be calculated following
304 Equation 7:

$$305 U_{AAE_{BC}} = t_p \times S(a) \quad (7)$$

306 Where $S(a)$ represents the standard deviation of the regression intercept (a) calculated

307 by the SPSS software, and t_p is determined by the t-distribution list according to a
308 confidence level (p), which was set to be 95% in this study.

309

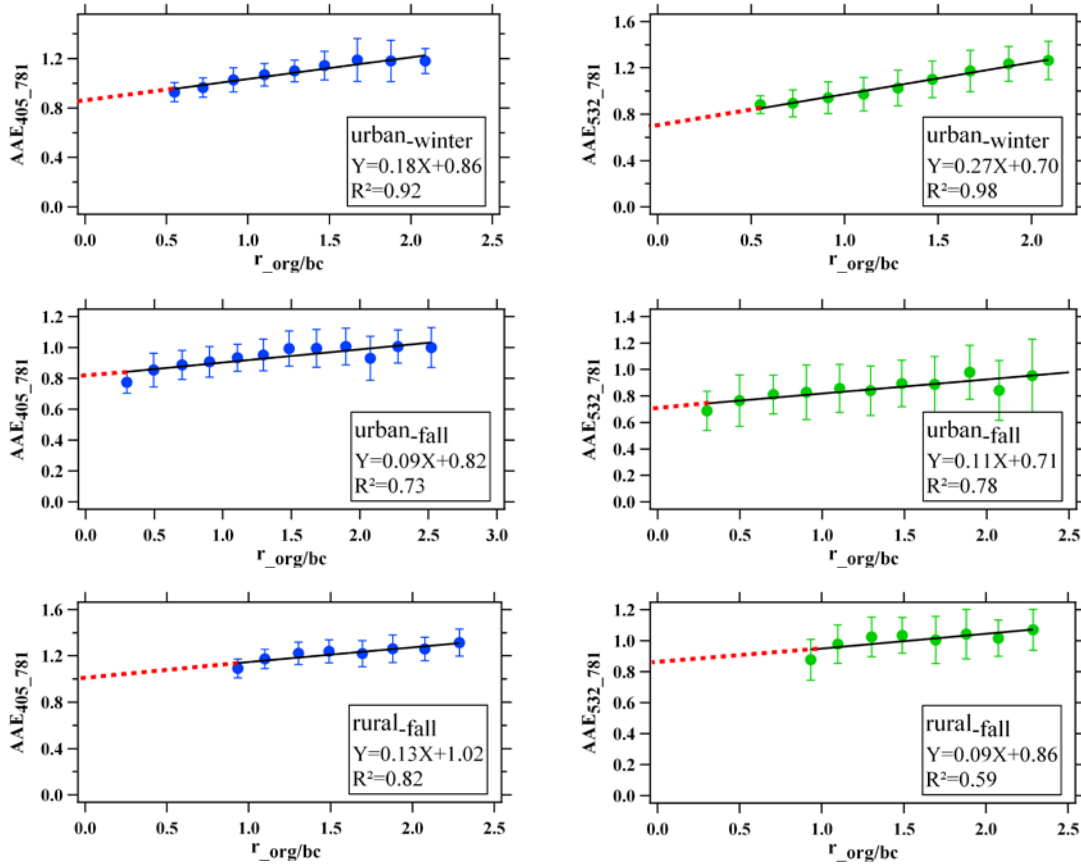
310 The calculated AAE_{BC} values and corresponding uncertainties at 405 and 532 nm
311 were summarized in Table 2, and they were found similar in the urban_{-winter}
312 (0.86 ± 0.06 and 0.70 ± 0.05) and urban_{-fall} (0.82 ± 0.06 and 0.71 ± 0.06) campaigns, but
313 were higher in the rural_{-fall} campaign (1.02 ± 0.10 and 0.86 ± 0.13). The difference of the
314 AAE_{BC} between the urban site and rural site might result from different sources of
315 BC aerosol. Fossil fuel combustion, e.g., vehicle emissions, was indicated to be the
316 dominant source of BC aerosol in urban Shenzhen (Lan et al., 2011), while biomass
317 burning emissions played an important role in the fall at the rural HS site (Gong et al.,
318 2012). In PRD, Lan (2013) ever found that the BC diameters of both vehicular
319 exhaust and biomass burning were generally above 100 nm, using a single particle
320 soot photometer to measure, and the BC diameters of vehicular emissions were even
321 larger. On the other hand, Gyawali et al. (2009) found that the AAE value would
322 decrease as the BC diameter increases in the range of 0.1–1 μm by theoretical
323 modeling. Therefore, the larger AAE_{BC} obtained at the rural site could be a result of
324 the smaller BC diameters of biomass burning in PRD.

325

326 It should be noted that previous studies showed that AAE of ambient aerosol can also
327 be influenced by a couple of other factors, such as size distribution, mixing state, and
328 fractal dimension of BC particles (Levin et al., 2010; Gyawali et al., 2009; Scarnatol
329 et al., 2013; Bond et al., 2006), but it is quite complicated and almost impossible to
330 consider the influence of all these factors simultaneously. Scarnato et al. (2013) also
331 pointed out that it is very difficult to clarify the relationship between AAE and aerosol
332 morphology and mixing state due to quite complicated mechanisms in real cases. In
333 this study, this issue was just simplified using a univariate regression analysis to
334 explore the relationship between ambient AAE and organic aerosol. In result, the
335 good correlations obtained in Fig. 2 indicated that BrC itself could be the dominant
336 factor leading to the variation of AAE, and thus the extrapolated intercept was a good

337 surrogate for AAE_{BC} . The influence of other factors could be partly reflected by the
 338 error bars of the data points in Fig. 2 and the estimated uncertainty of the intercept
 339 (i.e., $U_{AAE_{BC}}$).

340



341

342 **Fig.2.** The linear relationship between AAE and $r_{org/bc}$ in the different campaigns.

343

344 **Table 2.** The derived AAE_{BC} values and uncertainties in the different campaigns.

Campaign	AAE_{405_781}	AAE_{532_781}
Urban _{-winter}	0.86 ± 0.06	0.70 ± 0.05
Urban _{-fall}	0.82 ± 0.06	0.71 ± 0.06
Rural _{-fall}	1.02 ± 0.10	0.86 ± 0.13

345

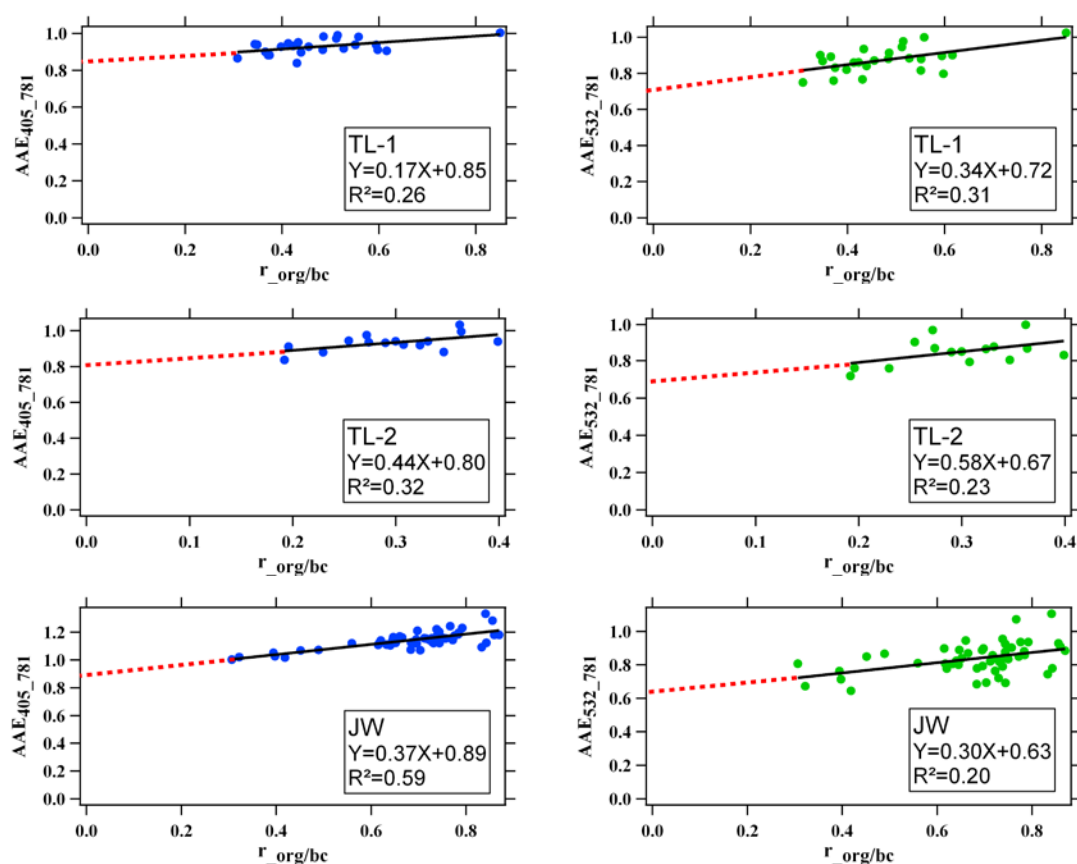
346 3.3 AAE measurements of primary emission sources

347 3.3.1 Roadway tunnel experiments

348 Since the major primary source of BC in urban environment in PRD was proved to be
 349 vehicular exhaust (Yuan et al., 2006; Huang et al., 2006; Lan et al., 2013), we
 350 performed three roadway tunnel experiments in urban Shenzhen, in order to verify the

351 representativeness of the AAE_{BC} derived from the urban atmosphere. The tunnel air
 352 measurement results were presented in Fig. 3. Since the tunnel air was largely
 353 dominated by fresh BC particles, the observed $r_{org/bc}$ values were found in a lower
 354 range (0.2–0.8) in comparison with those in the urban atmosphere, and thus the
 355 extrapolation of the linear regression in Fig. 3 could get more reliable intercepts, i.e.,
 356 AAE_{BC} . As summarized in Table 3, the AAE_{BC} values obtained at 405 and 532 nm
 357 (0.80–0.89 and 0.63–0.72, respectively) in the tunnel experiments well confirmed the
 358 AAE_{BC} values derived from the ambient measurements in urban Shenzhen.

359



360

361 **Fig.3.** The linear relationship between AAE and $r_{org/bc}$ in the tunnel experiments.

362

363

Table 3. The derived AAE_{BC} values and uncertainties in the tunnel experiments.

Tunnel	AAE_{405_781}	AAE_{532_781}
TL-1	0.85 ± 0.06	0.72 ± 0.10
TL-2	0.80 ± 0.11	0.68 ± 0.19
JW	0.89 ± 0.06	0.63 ± 0.12

364

365 3.3.2 Biomass burning simulation experiments

366 The AAE values with standard deviations of different types of biomass burning were
367 presented in Table 4. It was found that the absorption generally showed large spectral
368 dependence and the AAE varied among different biomass types or combustion modes,
369 with $AAE_{405-532}$ ranging from 2.1–8.3, $AAE_{532-781}$ ranging from 1.3–5.0, and
370 $AAE_{405-781}$ ranging from 1.7–6.2, significantly higher than those observed in the
371 ambient air and tunnel air. Therefore, the higher AAE values observed for biomass
372 burning particles, especially between 405 and 532 nm, proved that biomass burning
373 was a significant contributor to absorption at shorter wavelengths in the rural_{-fall}
374 campaign. In the combustion mode of stove burning, the leaves tended to emit more
375 BrC than wood, stalk, and straw, which should be a result of their different biomass
376 chemical nature. Besides, the AAE values of short straw were a few times higher in
377 open burning than in stove burning, which could be explained by that it was easier to
378 cause a hypoxic environment in smoldering and a larger amount of yellow fume was
379 produced (Einfeld et al., 1991; Patterson and McMahon, 1984; Kirchstetter et al.,
380 2004; Chakrabarty et al., 2010).

381

382 **Table 4.** The AAE values observed in the biomass burning simulation experiments.

Biomass type	Burning modes	$AAE_{405-532}$	$AAE_{532-781}$	$AAE_{405-781}$
Short straw	Open burning	8.27±1.34	4.96±1.15	6.20±1.33
Ficus microcarpa leaf	Stove burning	5.85±1.69	3.46±0.96	4.46±1.20
Lychee leaf	Stove burning	4.90±1.61	2.52±1.07	3.48±1.20
Corn stalk	Stove burning	3.83±1.49	2.39±1.06	2.97±1.16
Litchi wood	Stove burning	3.55±1.50	1.95±0.85	2.61±1.00
Eucalyptus wood	Stove burning	2.34±0.85	1.30±0.53	1.71±0.50
Short straw	Stove burning	2.32±0.65	1.39±0.47	1.76±0.25
Peanut stalk	Stove burning	2.13±1.01	2.08±0.86	1.99±0.50

383

384 3.4 Quantification of light absorption of BrC

385

386 Based on the well determined AAE_{BC} and Abs_{781nm} in the three field campaigns, we
387 could finally calculate the light absorption of BrC at 405 and 532 nm according to

388 Equation 3. In result, the average light absorption of BrC at 405 nm was 3.0, 1.4, and
389 3.9 Mm^{-1} in the urban_{-winter}, urban_{-fall}, and rural_{-fall} campaigns, respectively,
390 contributing 11.7%(±5%), 6.3%(±4%), and 12.1%(±7%) of the total aerosol light
391 absorption, respectively. Here, the values in the brackets were the relative
392 uncertainties calculated through Equation 4. The average light absorption of BrC at
393 532 nm was 1.9, 0.7, and 1.2 Mm^{-1} in the urban_{-winter}, urban_{-fall}, and rural_{-fall} campaigns,
394 respectively, contributing 10.0%(±2%), 4.1%(±3%), and 5.5%(±5%) of the total
395 aerosol light absorption, respectively.

396

397 The results indicated that no matter at the urban site or rural site in PRD, BC still
398 played a dominant role in total aerosol light absorption at 405 and 532 nm, but the
399 contribution of BrC was not negligible, with a fraction of up to 12%. The higher BrC
400 contribution in the urban_{-winter} campaign than that in the urban_{-fall} campaign suggested
401 that BrC could play a more important role in polluted continental air mass, since
402 Shenzhen had a higher frequency of continental air mass from the north than that of
403 marine air mass from the south in winter. On the other hand, the highest BrC
404 contribution at 405 nm in the rural_{-fall} campaign could be attributed to the influence of
405 biomass burning in the farmland nearby, which was supported by the biggest
406 difference of BrC absorption between 405 and 532 nm: the AAE_{405_532} of BrC was
407 calculated to be 1.7, 2.5, and 4.3 for the campaigns of urban_{-winter}, urban_{-fall}, and
408 rural_{-fall}, respectively. High AAE_{405_532} was found to be a feature in the biomass
409 burning simulation experiments, as in Table 4. Especially strong absorption at 404 nm
410 of biomass burning-emitted BrC was also found by Lack et al. (2012b). The lowest
411 AAE_{405_532} of the urban_{-winter} campaign indicated that fossil fuel combustion, rather
412 than biomass burning, seemed to be the major source of BrC in Shenzhen in winter.

413

414 Finally, it should be noted that it is unwise to calculate the light absorption
415 contribution of BrC at a specific time during the field campaigns, since the AAE_{BC}
416 derived for the whole case of a single campaign could have a large bias from the real
417 AAE_{BC} at that time, due to variations of the influencing factors, e.g., size distribution,

418 mixing state, and morphology of BC particles.

419

420 **4. Conclusions**

421

422 In this study, an improved AAE method was used to estimate the light absorption of
423 BrC at an urban site and a rural site in the PRD region of China in polluted seasons
424 during 2014, based on ambient on-line measurements using PASS-3 and AMS (or
425 ACSM). The obtained ambient $AAE_{405-781}$ averages were 1.05, 0.92, and 1.22 in the
426 three campaigns of urban_{winter}, urban_{fall}, and rural_{fall}, respectively, while those for
427 $AAE_{532-781}$ were 0.98, 0.82, and 1.00, respectively. The linear regression between
428 $AAE_{405-781}$ (or $AAE_{532-781}$) and the ratio of organic aerosol to BC resulted in
429 reasonable intercepts, which were assumed to be the AAE for “pure” BC (AAE_{BC}).
430 The obtained AAE_{BC} values between 405–781 nm were 0.86, 0.82, and 1.02 in the
431 campaigns of urban_{winter}, urban_{fall}, and rural_{fall}, respectively, and those between
432 532–781 nm were 0.70, 0.71, and 0.86, respectively. These AAE_{BC} values were
433 believed to be more realistic in PRD than the theoretical default value of 1.0. The
434 results of the tunnel experiments further confirmed that the realistic AAE_{BC} values in
435 the urban atmosphere should be within the ranges of 0.8–0.9 between 405 and 781 nm
436 and of 0.6–0.7 between 532 and 781 nm. In result, the average BrC light absorption
437 contributions (\pm relative uncertainties) at 405 nm were quantified to be 11.7% ($\pm 5\%$),
438 6.3% ($\pm 4\%$), and 12.1% ($\pm 7\%$) in the campaigns of urban_{winter}, urban_{fall}, and rural_{fall},
439 respectively, and those at 532 nm were 10.0% ($\pm 2\%$), 4.1% ($\pm 3\%$), and 5.5% ($\pm 5\%$),
440 respectively. It was found that BrC played a more important role in more polluted
441 winter or in the rural area with intensive biomass burning in PRD. Although BC still
442 played a dominant role in total aerosol light absorption in PRD, the contribution of
443 BrC at shorter wavelengths was not negligible, with a percent of up to $>10\%$.

444

445 **Acknowledgements**

446

447 This work was supported by the National Natural Science Foundation of China

448 (21277003 & U1301234), the Ministry of Science and Technology of China
449 (2013CB228503), and the Science and Technology Plan of Shenzhen Municipality.

450

451 **References**

452

453 Alexander, L., Julia, L., Serger, A. N.: Chemistry of Atmospheric Brown Carbon, Chemical Reviews., Special
454 Issue: Chemistry in Climate, 115, 4335-4382, DOI:10.1021/CR5006167,2015.

455 Ångström, A.: On the Atmospheric Transmission of Sun Radiation and on Dust in the Air, *Geografika Ann.*, 11,
456 156–166, 1929.

457 Arnott, W. P., Moosmuller, H., Rogers, C. F., Jin, T. F., Bruch, R.: Photoacoustic spectrometer for measuring light
458 absorption by aerosol: instrument description, *Atmos. Environ.*, 33, 2845–2852, 1999.

459 Arnott, W. P., Moosmuller, H., Walker, J. W.: Nitrogen Dioxide and Kerosene-Flame Soot Calibration of
460 Photoacoustic Instruments for Measurement of Light Absorption by Aerosols, *Rev. Sci. Instrum.*, 71,
461 4545–4552, doi: 10.1063/1.1322585, 2000.

462 Arola, A., Schuster, G., Myhre, G., Kazadzis, S., Dey, S., Tripathi, N.: Inferring absorbing organic carbon content
463 from AERONET data, *Atmos. Chem. Phys.*, 11, 215–225, doi:10.5194/acp-11-215-2011, 2011.

464 Bahadur, E., Praveen, P. S., Xu, Y., Ramanathan, V.: Solar absorption by elemental and brown carbon determined
465 from spectral observations, *P. Natl. Acad. Sci.*, 109, 17366–17371, 2012.

466 Bergstrom, R. W., Pilewskie, P., Russell, P. B., Redemann, J., Bond, T. C., Quinn, P. K., Sierau, B.: Spectral
467 absorption properties of atmospheric aerosols, *Atmos. Chem. Phys.*, 7, 5937–5943, 2007.

468 Bond, T. C., Bergstrom, R.W.: Light Absorption by Carbonaceous Particles: An Investigative Review, *Aerosol Sci.*
469 *Technol.*, 40(1), 27–67, doi:10.1080/02786820500421521, 2006.

470 Bond, T. C., Streets, D. G., Yarber, K. F., Nelson, S. M., Woo, J. H., Klimont, Z.: A technology-based global
471 inventory of black and organic carbon emissions from combustion, *J. Geophys. Res.*, 109, D14203.
472 doi:10.1029/2003jd003697, 2004.

473 Bond, T.C.: Spectral dependence of visible light absorption by carbonaceous particles emitted from coal
474 combustion, *Geophys. Res. Lett.*, 28, 4075–4078, 2001.

475 Chakrabarty, R. K., Arnold, I. J., Francisco, D. M., Hatchett, B., Hosseinpour, F., Loria, M., Pokharel, A., Woody,
476 B. M.: Black and brown carbon fractal aggregates from combustion of two fuels widely used in Asian rituals,
477 *Journal of Quantitative Spectroscopy & Radiative Transfer.*, 122, 25–30, doi:10.1016/j.jqsrt.2012.12.011, 2013.

478 Chakrabarty, R. K., Moosmuller, H., Chen, L. W. A., Lewis, K., Arnott, W. P., Mazzoleni, C., Dubey, M. K.,
479 Wold, C. E., Hao, W. M., Kreidenweis, S. M.: Brown carbon in tar balls from smoldering biomass combustion,
480 *Atmos. Chem. Phys.*, 10, 6363–6370, doi:10.5194/acp-10-6363-2010, 2010.

481 Chakrabarty, R. K., Pervez, S., Chow, J. C., Watson, J. G., Dewangan, S., Robles, J., Tian, G. X.: Funeral Pyres in
482 South Asia: Brown Carbon Aerosol Emissions and Climate Impacts, *Environ. Sci. Technol. Lett.*, 1, 44-48, doi:
483 10.1021/ez4000669, 2014.

484 Chen, Y., Bond, T. C.: Light absorption by organic carbon from wood combustion, *Atmos. Chem. Phys.*, 10,
485 1773-1787, 2010.

486 Chung, C. E., Kim, S. W., Lee, M., Yoon, S. C., Lee, S.: Carbonaceous aerosol AAE inferred from in-situ aerosol
487 measurements at the Gosan ABC super site, and the implications for brown carbon aerosol, *Atmos. Chem.*
488 *Phys.*, 12, 6173–6184, doi:10.5194/acp-12-6173-2012, 2012a.

489 Chung, C. E., Ramanathan, V., Decremer, D.: Observationally constrained estimates of carbonaceous aerosol
490 radiative forcing, *P. Natl. Acad. Sci.*, 109(29), 11624-11629, 2012b.

491 Clarke, A., McNaughton, C., Kapustin, V., Shinozuka, Y., Howell, S., Dibb, J., Zhou, J., Anderson, B.,
492 Brekhovskikh, V., Turner, H., and Pinkerton, M.: Biomass Burning and Pollution Aerosol over North America:
493 Organic Components and Their Influence on Spectral Optical Properties and Humidification Response, *J.*
494 *Geophys. Res.*, 112, D12S18, doi: 10.1029/2006jd007777, 2007.

495 DeCarlo, P. F., Kimmel, J. R., Trimborn, A., Northway, M. J., Jayne, J. T., Aiken, A. C., Gonin, M., Fuhrer, K.,
496 Horvath, T., Docherty, K. S., Worsnop, D. R., Jimenez, J. L.: Field-Deployable, High-Resolution
497 Time-of-Flight Aerosol Mass Spectrometer, *Anal. Chem.*, 78, 8281–8289, 2006.

498 Drewnick, F., Hings, S. S., DeCarlo, P., Jayne, J. T., Gonin, M., Fuhrer, K., Weimer, S., Jimenez, J. L., Demerjian,
499 K. L., Borrmann, S., Worsnop, D. R.: A new time-of-flight aerosol mass spectrometer (TOF-AMS)–Instrument
500 description and first field deployment, *Aerosol. Sci. Tech.*, 39, 637–658, 2005.

501 Einfeld, W., Ward, D. E., and Hardy, C.: Effects of fire behavior on prescribed fire smoke characteristics: A case
502 study, in: *Global biomass burning: Atmospheric, climatic, and biospheric implications*, MIT Press, Cambridge,
503 MA, USA, 412–419, 1991.

504 Favez, O., Alfaro, S. C., Sciare, J., Cachier, H., Abdelwahab, M. M.: Ambient measurements of light-absorption
505 by agricultural waste burning organic aerosols, *J. Aerosol. Sci.*, 40, 613–620, 2009.

506 Feng, Y., Ramanathan, V., Kotamarthi, V. R.: Brown carbon: a significant atmospheric absorber of solar radiation?
507 *Atmos. Chem. Phys.*, 13(17), 8607-8621, 2013.

508 Gadhavi, H., Jayaraman, A.: Absorbing aerosols: contribution of biomass burning and implications for radiative
509 forcing, *Ann. Geophys.*, 28, 103–111, doi:10.5194/angeo-28-103-2010, 2010.

510 Gong, Z. H., Lan, Z. J., Xue, L., Zeng, L. W., He, L. Y., Huang, X. F.: Characterization of submicron aerosols in
511 the urban outflow of the central Pearl River Delta region of China, *Environ. Sci. Eng.*, 6(5): 725–733, 2012.

512 Gyawali, M., Arnott, W. P., Lewis, K., Moosmüller, H.: In situ aerosol optics in Reno, NV, USA during and after
513 the summer 2008 California wildfires and the influence of absorbing and non-absorbing organic coatings on
514 spectral light absorption, *Atmos. Chem. Phys.*, 9, 8007–8015, doi:10.5194/acp-9-8007-2009, 2009.

515 Hansen, J., Sato, M., Ruedy, R.: Radiative forcing and climate response, *J. Geophys. Res.*, 102, 6831-6864, 1997.

516 Haywood, J. M., Roberts, D. L., Slingo, A., Edwards, J. M., Shine, K. P.: General circulation model calculations of
517 the direct radiative forcing by anthropogenic sulfate and fossil-fuel soot aerosol, *Journal of Climate.*, 10,
518 1562-1577, 1997.

519 He, L. Y., Huang, X. F., Xue, L., Hu, M., Lin, Y., Zheng, J., Zhang, R. Y., Zhang, Y. H.: Submicron aerosol
520 analysis and organic source apportionment in an urban atmosphere in Pearl River Delta of China using

521 high-resolution aerosol mass spectrometry, *J. Geophys. Res.*, 116 (D12304), DOI: 10.1029/2010JD014566,
522 2011.

523 He, L. Y., Lin, Y., Huang, X. F., Guo, S., Xue, L., Sun, Q., Hu, M., Luan, S. J., Zhang, Y. H.: Characterization of
524 high-resolution aerosol mass spectra of primary organic aerosol emissions from Chinese cooking and biomass
525 burning, *Atmos. Chem. Phys.*, 10, 11535–11543, 2010.

526 He, M., Zheng, J. Y., Yin, S. S., Zhang, Y. Y.: Trends, temporal and spatial characteristics, and uncertainties in
527 biomass burning emissions in the Pearl River Delta, China, *Atmos. Environ.*, 45, 4051–4059,
528 doi:10.1016/j.atmosenv.2011.04.016, 2011.

529 Huang, X. F., He, L. Y., Hu, M., Canagaratna, M. R., Kroll, J. H., Ng, N. L., Zhang, Y. H., Lin, Y., Xue, L., Sun,
530 T. L., Liu, X. G., Shao, M., Jayne, J. T., Worsnop, D. R.: Characterization of submicron aerosols at a rural site
531 in Pearl River Delta of China using an aerodyne high-resolution aerosol mass spectrometer, *Atmos. Chem.*
532 *Phys.*, 11(5): 1865–1877, 2011.

533 Huang, X. F., Sun, T. L., Zeng, L. W., Yu, G. H., Luan, S. J.: Black carbon aerosol characterization in a coastal
534 city in South China using a single particle soot photometer, *Atmos. Environ.*, 51, 21–28, 2012.

535 Huang, X. F., Yun, H., Gong, Z. H., Li, X., He, L. Y., Zhang, Y. H., Hu, M.: Source apportionment and secondary
536 organic aerosol estimation of PM_{2.5} in an urban atmosphere in China, *Science China: Earth Sciences.*, 57,
537 1352–1362, 2014.

538 Jacobson, M. Z.: Isolating nitrated and aromatic aerosols and nitrated aromatic gases as sources of ultraviolet light
539 absorption. *J. Geophys. Res.*, 104:3527–3542, 1999.

540 Jacobson, M. Z.: Strong radiative heating due to the mixing state of black carbon in atmospheric aerosols, *Nature*
541 409, 695–697, 2001.

542 Jayne, J. T., Leard, D. C., Zhang, X. F., Davidovits, P., Smith, K. A., Kolb, C. E., Worsnop, D. R.: Development
543 of an aerosol mass spectrometer for size and composition analysis of submicron particles, *Aerosol. Sci. Tech.*,
544 33, 49–70, 2000.

545 Jethva, H., Torres, O.: Satellite-based evidence of wavelength-dependent aerosol absorption in biomass burning
546 smoke inferred from Ozone Monitoring Instrument, *Atmos. Chem. Phys.*, 11, 10541–10551,
547 doi:10.5194/acp-11-10541-2011, 2011.

548 Jimenez, J. L., Jayne, J. T., Shi, Q., Kolb, C. E., Worsnop, D. R., Yourshaw, I., Seinfeld, J. H., Flagan, R. C.,
549 Zhang, X. F., Smith, K. A., Morris, J. W., Davidovits, P.: Ambient aerosol sampling using the Aerodyne
550 Aerosol Mass Spectrometer, *J. Geophys. Res.*, 108, 8425, D7, doi:10.1029/2001JD001213, 2003.

551 Kirchstetter, T. W., Novakov, T., Hobbs, P. V.: Evidence that the spectral dependence of light absorption by
552 aerosols is affected by organic carbon. *J. Geophys. Res.*, 109, D21, doi:10.1029/2004JD004999, 2004.

553 Koch, D., Hansen, J.: Distant origins of Arctic black carbon: a Goddard Institute for Space Studies ModelE
554 experiment, *J. Geophys. Res.*, 110, D04204, doi:10.1029/2004jd005296, 2005.

555 Lack, D. A., Cappa, C. D., Cross, E. S., Massoli, P., Ahern, A. T., Davidovits, P., Onasch, T. B. : Absorption
556 Enhancement of Coated Absorbing Aerosols: Validation of the Photo-Acoustic Technique for Measuring the
557 Enhancement, *Aerosol Sci. Tech.*, 43, 1006–1012, 2009.

558 Lack, D. A., Langridge, J. M., Bahreini, R., Cappa, C. D., Middlebrook, A. M., and Schwarz, J. P.: Brown carbon
559 and internal mixing in biomass burning particles, *P. Natl. Acad. Sci. USA.* 109, 37, 14802-14807,
560 doi:10.1073/pnas.1206575109, 2012b.

561 Lack, D. A., Langridge, J. M.: On the attribution of black and brown carbon light absorption using the Ångström
562 exponent, *Atmos. Chem. Phys.*, 13, 5089–5101, 2013.

563 Lack, D. A., Langridge, J., Richardson, M., Cappa, C. D., Law, D., Murphy, D. M.: Aircraft instrumentation for
564 comprehensive characterization of aerosol optical properties, Part 2: Black and brown carbon absorption and
565 absorption enhancement measured with photo acoustic spectroscopy, *Aerosol Sci. Tech.*, 46, 555–568, 2012a.

566 Lack, D. A., Moosmüller, H., McMeeking, G. R., Chakrabarty, R. K., Baumgardner, D.: Characterizing elemental,
567 equivalent black, and refractory black carbon aerosol particles: a review of techniques, their limitations and
568 uncertainties, *Anal Bioanal Chem.*, 406:99–122, doi:10.1007/s00216-013-7402-3, 2014.

569 Lan, Z. J., Chen, D. L., Li, X., Huang, X. F., He, L. Y., Deng, Y. G., Feng, N., Hu, M.: Modal characteristics of
570 carbonaceous aerosol size distribution in an urban atmosphere of South China, *Atmospheric Research.*, 100,
571 51-60, 2011.

572 Lan, Z. J., Huang, X. F., Yu, K. Y., Sun, T. L., Zeng, L. W., Hu, M.: Light absorption of black carbon aerosol and
573 its enhancement by mixing state in an urban atmosphere in South China, *Atmos. Environ.*, 69,118-123, 2013.

574 Lan, Z. J.: Characteristics of mixing state and light absorption of black carbon aerosol in China, PhD dissertation,
575 Peking University., 2013.

576 Levin, E. J. T., McMeeking, G. R., Carrico, C. M., Mack, L. E., Kreidenweis, S. M. Word, C. E., Moosmuller, H.,
577 Arnott, W. P., Hao, W. M., Cottett Jr, J. L., Malm, W. C.: Biomass burning smoke aerosol properties measured
578 during Fire Laboratory at Missoula Experiments (FLAME), *J. Geophys. Res.*, Atmos 115:D182010, DOI:
579 10.1029/2009JD013601, 2010.

580 Lewis, K., Arnott, W. P., Moosmuller, H., Wold, C. E.: Strong spectral variation of biomass smoke light
581 absorption and single scattering albedo observed with a novel dual-wavelength photoacoustic instrument, *J.*
582 *Geophys. Res.*, 113, D16, DOI: 10.1029/2007JD009699, 2008.

583 Moosmuller, H., Arnott, W. P., Rogers, C. F., Chow, J. C., Frazier, C. A., Sherman, L. E., Dietrich, D. L.:
584 Photoacoustic and filter measurements related to aerosol light absorption during the Northern Front Range Air
585 Quality Study (Colorado 1996/1997), *J. Geophys. Res.*, 103(D21), 28149-28157, 1998.

586 Nakayama, T., Ikeda, Y., Sawada, Y., Setoguchi, Y., Ogawa, S., Kawana, K., Mochida, M., Ikemori, F.,
587 Matsumoto, K., Matsumi, Y.: Properties of light-absorbing aerosols in the Nagoya urban area, Japan, in August
588 2011 and January 2012: Contributions of brown carbon and lensing effect, *J. Geophys. Res. Atmos.*, 119,
589 12,721–12,739, doi:10.1002/ 2014JD021744, 2014.

590 Nakayama, T., Suzuki, H., Kagamitani, S., Ikeda, Y.: Characterization of a three wavelength photoacoustic soot
591 spectrometer (PASS-3) and photoacoustic extinciometer (PAX), *J. Meteorol. Soc. Jpn.*, 93, 285–308, doi:
592 10.2151/jmsj.2015-016, 2015.

593 Ng, N. L., Herndon, S. C., Trimborn, A., Canagaratna, M. R., Croteau, P. L., Onasch, T. B., Sueper, D., Worsnop,
594 D. R., Zhang, Q., Sun, Y. L., Jayne, J. T.: An Aerosol Chemical Speciation Monitor (ACSM) for routine
595 monitoring of the composition concentrations of ambient aerosol, *Aerosol Sci. Tech.*, 45, 770-784, 2011..

596 Patterson, E. M., McMahon, C. K.: Absorption characteristics of forest fire particulate matter, *Atmos. Environ.*, 18,
597 2541–2551, 1984.

598 Poschl, U.: Atmospheric Aerosols: Composition, Transformation, Climate, and Health Effects, *Atoms. Chem.*, 44,
599 7520-7540, 2005.

600 Ramanathan, V., Carmichael, G.: Global and regional climate changes due to black carbon, *Nature Geoscience.*, 1,
601 221-227, 2008.

602 Ramanathan, V., Ramana, M.V., Roberts, G., Kim, D., Corrikanm, C., Chung, C., Winker, D.: Warming trends in
603 Asia amplified by brown cloud solar absorption. *Nature* 448, 575-578, doi:10.1038/nature06019 , 2007.

604 Sandradewi, J., Prevot, A. S. H., Weingartner, E., Schmidhauser, R., Gysel, M., Baltensperger, U.: A study of
605 wood burning and traffic aerosols in an Alpine valley using a multi-wavelength Aethalometer, *Atmos.*
606 *Environ.*,42, 101-111, 2008.

607 Scarnato, B. V., Vahidinal, S., Richard, D. T., Kirchstetter, T. W.: Effects of internal mixing and aggregate
608 morphology on optical properties of black carbon using a discrete dipole approximation model, *Atmos. Chem.*
609 *Phys.*, 13, 5089–5101, 2013.

610 Schmid, O., Artaxo, P., Arnott, W. P., Chand, D., Gatti, L. V., Frank, G. P., Hoffer, A., Schnaiter, M., Andreae, M.
611 O.: Spectral light absorption by ambient aerosols influenced by biomass burning in the Amazon Basin. I:
612 comparison and field calibration of absorption measurement techniques. *Atmos. Chem. Phys.*, 6, 3443-3462,
613 2006.

614 Streets, D. G., Gupta, S., Waldhoff, S. T., Wang, M. Q., Bond, T. C., Bo, Y. Y.: Black carbon emissions in China,
615 *Atmos. Environ.*, 35, 4281-4296, 2001.

616 Sun, H., Biedermann, L., Bond, T. C.: Color of brown carbon: A model for ultraviolet and visible light absorption
617 by organic carbon aerosol, *Geophys. Res. Lett.*, 34:L17813, DOI:10.1029/2007GL029797, 2007.

618 Utry, N., Ajtai, T., Pinter, M., Torok, Z., Bozoki, Z., Szabo, G.: Correlations between absorption Angström
619 exponent (AAE) of wintertime ambient urban aerosol and its physical and chemical properties, *Atmos.*
620 *Environ.*, 91, 52-59, doi: 10.1016/j.atmosenv.2014.03.047, 2014

621 Venkataraman, C., Habib, G., Kadamba, D., Shrivastava, M., Leon, J.-F., Crouzille, B., Boucher, O., Streets, D. G.:
622 Emissions from open biomass burning in India: Integrating the inventory approach with high-resolution
623 Moderate Resolution Imaging Spectroradiometer (MODIS) active-fire and land cover data, *Global*
624 *Biogeochemical Cycles.*, 20, GB2013, doi:10.1029/2005GB002547, 2006.

625 Wang, X., Heald, C. L., Ridley, D. A., Schwarz, J. P., Spackman, J. R., Perring, A. E., Clarke, A. D.: Exploiting
626 simultaneous observational constraints on mass and absorption to estimate the global direct radiative forcing of
627 black carbon and brown carbon, *Atmos. Chem. Phys.*, 14(20), 10989-11010, 2014.

628 Washenfelder, R. A., Attwood, A. R., Brock, C. A., Guo, H., Xu, L., Weber, R. J., Ng, N. L., Allen, H. M., Ayres,
629 B. R., Baumann, K., Cohen, R. C., Draper, D. C., Duffey, K. C., Edgerton, E., Fry, J. L., Hu, W. W., Jimenez, J.
630 L., Palm, B. B., Romer, P., Stone, E. A., Wooldridge, P. J., Brown, S. S.: Biomass burning dominates brown
631 carbon absorption in the rural southeastern United States, *Geophys. Res. Lett.*, 42, 653-664, DOI:
632 10.1002/2014GL062444, 2015.

633 Yan, X. Y., Ohara, T., Akimoto, H.: Bottom-up estimate of biomass burning in mainland China, *Atmos. Environ.*,

- 634 40, 5262-5273, doi:10.1016/j.atmosenv.2006.04.040, 2006.
- 635 Yang, M., Howell, S. G., Zhuang, J., Huebert, B. J.: Attribution of aerosol light absorption to black carbon, brown
636 carbon, and dust in China – interpretations of atmospheric measurements during EAST-AIRE, *Atmos. Chem.*
637 *Phys.*, 9, 2035–2050, doi:10.5194/acp-9-2035-2009, 2009.
- 638 Yuan, Z. B., Lau, A. K. H., Zhang, Y. H., Yu, J. Z., Louie, P. K. K., Fung, J. C. H.: Identification and
639 spatiotemporal variations of dominant PM10 sources over Hong Kong, *Atmos. Environ.*, 40: 1803–1815, 2006.
- 640 Zhang, Y. H., Hu, M., Liu, S. C., Wiedensohler, A.: The special issue on PRIDE-PRD2004 campaign, *Atmos.*
641 *Environ.*, 42 (25): 6155–6156, 2008.
- 642 Zhang, Y. S., Shao, M., Lin, Y., Luan, S. J., Mao, N., Chen, W. T., Wang, M.: Emission inventory of
643 carbonaceous pollutants from biomass burning in the Pearl River Delta Region, China, *Atmos. Environ.*, 76,
644 189-199, doi: 10.1016/j.atmosenv.2012.05.055, 2013.